

PREPARED FOR SUBMISSION TO JHEP

Next-to-next-to-leading order threshold soft function for tW production

Jia-Le Ding^a, Hai Tao Li^a, and Jian Wang^{a,b}

^a*School of Physics, Shandong University, Jinan, Shandong 250100, China*

^b*Center for High Energy Physics, Peking University, Beijing 100871, China*

E-mail: dingjl@mail.sdu.edu.cn, haitao.li@sdu.edu.cn,
j.wang@sdu.edu.cn

ABSTRACT: We compute the two-loop soft function for the associated production of a top quark and a W boson near the threshold, where the invariant mass of the tW system approaches the collider energy. We employ the reverse unitarity technique and integration-by-parts identities to reduce soft loop integrals to a minimal basis of master integrals. These master integrals are analytically evaluated using the method of differential equations, yielding results expressed in terms of multiple polylogarithms. Additionally, we analyze the asymptotic behavior of the soft function in the low and high energy limits. Our results provide a vital component for threshold resummation at the next-to-next-to-next-to-leading logarithmic level in this process.

Contents

1	Introduction	1
2	Factorization of the cross section near threshold	2
3	NLO soft function	5
4	NNLO soft function	8
5	Asymptotic expansions and numerical results	12
6	Conclusions	15

1 Introduction

As the heaviest particle in the Standard Model (SM), the top quark plays an important role in both the precise test of the SM and searches for new physics. Among the various production modes of a single top quark, the associated production of a top quark with a W boson has the second-largest cross section at the Large Hadron Collider (LHC). The cross section for tW production is directly proportional to the square of the Cabibbo-Kobayashi-Maskawa (CKM) matrix element V_{tb} . Inclusive and differential cross sections for tW production have been measured extensively at the LHC [1–10], and all measurements agree well with theoretical predictions.

The tW production is particularly interesting due to its interference with the top quark pair production, which makes this process contain rich phenomenology in experiments [11]. Simultaneously, the interference leads to difficulties in making precise theoretical predictions. Substantial efforts have been dedicated to disentangling the tW signals from $t\bar{t}$ production and addressing interference effects at tree level [12–16] and one-loop level [17].

The next-to-leading order (NLO) quantum chromodynamics (QCD) corrections to tW production have been known for nearly three decades [14, 18–20]. Additionally, the contributions from soft-gluon radiation have been explored through higher-order expansions [21–24], and an all-order resummation within the Soft-Collinear Effective Theory (SCET) framework has been performed [25]. A combination of the NLO QCD calculation and the parton showers at NLO was provided by [15, 26, 27].

Progress toward next-to-next-to-leading order (NNLO) QCD corrections includes calculations of the two-loop hard function [28–33] and the two-loop N -jettiness soft function [34, 35]. Despite these advances, a complete NNLO QCD correction for tW production remains an open challenge.

In this paper, we present the calculation of the two-loop soft function for tW production in the threshold limit, where the invariant mass of the tW pair is close to the collider

energy. In this limit, the cross section can be factorized as a convolution of the parton distribution functions (PDFs), the hard function and the soft function. The complete two-loop soft function is an indispensable ingredient for next-to-next-to-next-to-leading logarithmic resummation of the soft gluon effects, which can be used to improve the theoretical accuracy near the threshold region. In the calculation, we make use of the reverse unitary method [36, 37] to convert the phase space constraint into the form of propagators. The soft integrals are reduced to a set of master integrals by integration-by-part (IBP) [38, 39] identities using FIRE6 [40] and the master integrals are calculated with the method of differential equations [41–44]. The final results are given in terms of multiple polylogarithms (MPLs) [45].

The rest of this paper is organized as follows. In section 2, we discuss the factorization of the cross section near the threshold. The calculations of the NLO and NNLO soft functions are presented in section 3 and section 4, respectively. In section 5, we explore the asymptotic behavior of the soft function in the low- and high-energy limits. Finally, we conclude in section 6.

2 Factorization of the cross section near threshold

The process we are considering is $b/\bar{b}(p_1) + g(p_2) \rightarrow t/\bar{t}(p_3) + W^-/W^+(p_4)$ where p_3 and p_4 denote the momenta of the outgoing top/anti-top quark and W boson, respectively, which satisfy $p_3^2 = m_t^2$ and $p_4^2 = m_W^2$. We introduce the light-cone vectors v_1 and v_2

$$v_1^\mu = (1, 0, 0, 1), \quad v_2^\mu = (1, 0, 0, -1), \quad (2.1)$$

which are along with the directions of p_1 and p_2 , respectively. The direction of the top quark momentum is expressed as

$$v_3^\mu = (1, 0, \beta \sin \theta, \beta \cos \theta), \quad (2.2)$$

where β is the velocity of the top quark and θ is the polar angle of the momentum of the top quark¹. Explicitly, the momenta of colored particles in this process are given by

$$p_1^\mu = \frac{\sqrt{s_{12}}}{2} v_1^\mu, \quad p_2^\mu = \frac{\sqrt{s_{12}}}{2} v_2^\mu, \quad p_3^\mu = \frac{m_t}{\sqrt{1-\beta^2}} v_3^\mu, \quad (2.3)$$

with $s_{12} = (p_1 + p_2)^2$.

In the threshold region, the invariant mass Q of the tW system is close to the hadronic energy of the collider, \sqrt{S} . This region is described by the hadronic threshold variable $R \rightarrow 0$ with

$$R = 1 - \frac{Q^2}{S} = 1 - \frac{x_1 x_2 Q^2}{s_{12}} = \frac{s_{12} - (1 - \Delta x_1)(1 - \Delta x_2) Q^2}{s_{12}} = \tau + \Delta x_1 + \Delta x_2, \quad (2.4)$$

where x_i are the momentum fractions of the initial-state partons in the protons and $\Delta x_i = 1 - x_i$. The partonic threshold variable τ is defined by

$$\tau = 1 - \frac{Q^2}{s_{12}} = \frac{(p_t + p_W + p_\omega)^2 - (p_t + p_W)^2}{s_{12}} = \frac{2E_\omega}{\sqrt{s_{12}}} \equiv \frac{\omega}{\sqrt{s_{12}}}, \quad (2.5)$$

¹Note that the θ angle in this soft function is different from that used in the hard function [32].

where p_ω^μ denotes the momentum sum of all soft radiations and $E_\omega = p_\omega^0$ is the energy in the partonic center-of-mass frame. It is clear that the hadronic threshold cannot be approached at any real colliders. However, the partonic threshold region can still be enhanced because the parton distribution functions drop fast at high x_i [46]. Therefore, the threshold contribution is dominant in the higher-order corrections as we show in ref. [25].

In the hadronic threshold limit, the cross section takes a factorization form [25],

$$\begin{aligned} \frac{d\sigma}{dRd\Phi_2} &= \int_0^1 dx_1 f_1(x_1, \mu) \int_0^1 dx_2 f_2(x_2, \mu) \frac{1}{2x_1 x_2 S} \times H(\mu, \beta, y) \\ &\times \int_0^\infty d\tau s(\tau, \mu, \beta, y) \delta(R - \tau - \Delta x_1 - \Delta x_2), \end{aligned} \quad (2.6)$$

where $d\Phi_2$ denotes the two-body phase space and $y \equiv \cos\theta$. $f_i(x_i, \mu)$ represent the PDFs with the momentum fractions x_i at the scale μ . H and s are the hard function and soft function, which describe the interactions at the hard and soft scales, respectively. In momentum space the soft function is defined as the vacuum matrix element

$$\begin{aligned} s(\tau, \mu, \beta, y) &= \sqrt{s_{12}} \int \frac{dx_0}{4\pi} e^{\frac{i\sqrt{s_{12}}\tau x_0}{2}} \times \\ &\sum_{X_s} \langle 0 | \bar{T} \{ Y_{v_1}^\dagger Y_{v_2} Y_{v_3} \} (x) | X_s \rangle \langle X_s | T \{ Y_{v_1} Y_{v_2}^\dagger Y_{v_3}^\dagger \} (0) | 0 \rangle \\ &= \sum_{X_s} \langle 0 | \bar{T} \{ Y_{v_1}^\dagger Y_{v_2} Y_{v_3} \} (0) | X_s \rangle \delta\left(\tau - \frac{v_0 \cdot \hat{p}_{X_s}}{\sqrt{s_{12}}}\right) \langle X_s | T \{ Y_{v_1} Y_{v_2}^\dagger Y_{v_3}^\dagger \} (0) | 0 \rangle \end{aligned} \quad (2.7)$$

with $x = (x_0, 0, 0, 0)$, $v_0 = v_1 + v_2$ and \hat{p}_{X_s} extracting all the momenta of the final-state soft particles. $T(\bar{T})$ is the (anti-)time-ordering operator, and $Y_{v_1}, Y_{v_2}^\dagger$ and $Y_{v_3}^\dagger$ are the soft Wilson lines defined by [47–49]

$$Y_{v_1}(x) = P \exp \left(-ig_s \int_{-\infty}^0 ds v_1 \cdot A_s^a(x + sv_1) \mathbf{T}_1^a \right), \quad (2.8)$$

$$Y_{v_2}^\dagger(x) = \bar{P} \exp \left(-ig_s \int_{-\infty}^0 ds v_2 \cdot A_s^a(x + sv_2) \mathbf{T}_2^a \right), \quad (2.9)$$

$$Y_{v_3}^\dagger(x) = P \exp \left(ig_s \int_0^{+\infty} ds v_3 \cdot A_s^a(x + sv_3) \mathbf{T}_3^a \right), \quad (2.10)$$

where $P(\bar{P})$ is the (anti-)path-ordering operator² and \mathbf{T}_i represents the color charge associating with the i -th parton [50, 51]³. For the initial- and final-state quark, the color-charge matrix is given by $\mathbf{T}_{ij}^a = -t_{ji}^a$ and $\mathbf{T}_{ij}^a = t_{ij}^a$, respectively. For the gluon, the color-charge matrix is $\mathbf{T}_{bc}^a = -if_{abc}$. Note that the color charge operators along different directions

²The (anti-)path-ordering operator rearranges the fields in such a way that the fields with higher values of s are to the left (right).

³Because we have used the color charge, the explicit forms of the soft Wilson lines may be different from the others used in previous literature.

commutate with each other, such as $[\mathbf{T}_1^a, \mathbf{T}_2^b] = 0$. As a result, the relative ordering of the Wilson lines $Y_{v_1}, Y_{v_2}^\dagger$ and $Y_{v_3}^\dagger$ in eq. (2.7) can be arbitrary.

It is convenient to perform the Laplace transformation

$$\begin{aligned}\frac{d\tilde{\sigma}(t, \mu)}{d\Phi_2} &= \int_0^\infty dR \frac{d\sigma}{dR d\Phi_2} \exp\left(-\frac{R}{t}\right), \\ \tilde{f}_i(t, \mu) &= \int_0^1 dx_i f_i(x_i, \mu) \exp\left(-\frac{1-x_i}{t}\right), \\ \tilde{s}(t, \mu, \beta, y) &= \int_0^\infty d\tau s(\tau, \mu, \beta, y) \exp\left(-\frac{\tau}{t}\right),\end{aligned}\tag{2.11}$$

which converts the cross section to a product of the PDFs, hard function and soft function,

$$\frac{d\tilde{\sigma}(t, \mu)}{d\Phi_2} = \frac{1}{2s_{12}} H(\mu, \beta, y) \tilde{f}_1(t, \mu) \tilde{f}_2(t, \mu) \tilde{s}(t, \mu, \beta, y). \tag{2.12}$$

Because the cross section is scale invariant, the renormalization group (RG) evolutions of the various components in eq. (2.12) satisfy the identity below order-by-order in the strong coupling α_s ,

$$\frac{d \ln H(\mu, \beta, y)}{d \ln \mu} + \frac{d \ln \tilde{f}_1(t, \mu)}{d \ln \mu} + \frac{d \ln \tilde{f}_2(t, \mu)}{d \ln \mu} + \frac{d \ln \tilde{s}(t, \mu, \beta, y)}{d \ln \mu} = 0. \tag{2.13}$$

Therefore, the soft anomalous dimension can be derived from the independence of the cross section on the renormalization scale μ ,

$$\gamma_s = \frac{d \ln \tilde{s}}{d \ln \mu} = -\frac{d \ln H}{d \ln \mu} - \frac{d \ln \tilde{f}_1}{d \ln \mu} - \frac{d \ln \tilde{f}_2}{d \ln \mu}. \tag{2.14}$$

The RG equation of the hard function can be obtained from the universal anomalous dimensions; see ref. [52]. The RG evolution of the PDFs in the threshold limit can be found in refs. [53, 54]. According to eq. (2.14), the anomalous dimension of the soft function is given by

$$\begin{aligned}\gamma_s &= -(\mathbf{T}_1^2 + \mathbf{T}_2^2) \gamma_{\text{cusp}} \left(\ln t^2 + \ln \frac{s_{12}}{\mu^2} \right) + \mathbf{T}_1 \cdot \mathbf{T}_3 \gamma_{\text{cusp}} \ln \frac{(1-\beta y)^2}{1-\beta^2} \\ &\quad + \mathbf{T}_2 \cdot \mathbf{T}_3 \gamma_{\text{cusp}} \ln \frac{(1+\beta y)^2}{1-\beta^2} - 2\gamma^q - 2\gamma^g - 2\gamma^Q - 2\gamma_f^q - 2\gamma_f^g,\end{aligned}\tag{2.15}$$

where all anomalous dimensions can be found in ref. [55]. The renormalized soft function reads

$$\tilde{s}(t, \mu, \beta, y) = Z_s^{-1} \tilde{s}_{\text{bare}}(t, \mu, \beta, y). \tag{2.16}$$

Because the bare soft function is scale independent, the renormalization constant Z_s satisfies the evolution equation

$$\frac{d \ln Z_s}{d \ln \mu} = -\gamma_s. \tag{2.17}$$

Solving this equation in the $\overline{\text{MS}}$ scheme, we obtain

$$\ln Z_s = \frac{\alpha_s}{4\pi} \left(\frac{\gamma_s'^{(0)}}{4\epsilon^2} + \frac{\gamma_s^{(0)}}{2\epsilon} \right) + \left(\frac{\alpha_s}{4\pi} \right)^2 \left(-\frac{3\beta_0\gamma_s'^{(0)}}{16\epsilon^3} + \frac{\gamma_s'^{(1)} - 4\beta_0\gamma_s^{(0)}}{16\epsilon^2} + \frac{\gamma_s^{(1)}}{4\epsilon} \right) + \mathcal{O}(\alpha_s^3), \quad (2.18)$$

where we have worked in $d = 4 - 2\epsilon$ dimensional spacetime to regulate the divergences and adopted the perturbative expansion in α_s ,

$$\gamma_s = \sum_{i=0} \left(\frac{\alpha_s}{4\pi} \right)^{i+1} \gamma_s^{(i)}. \quad (2.19)$$

We have also used the notation $\gamma_s' = \partial\gamma_s/\partial\ln\mu$ and $\beta_0 = 11C_A/3 - 2n_f/3$ with $C_A = 3$ and n_f being the number of active quark flavors.

After expanding eq. (2.16) order-by-order in $\alpha_s/4\pi$, the renormalized NLO and NNLO soft functions in Laplace space are given by

$$\tilde{s}^{(1)} = \tilde{s}_{\text{bare}}^{(1)} - Z_s^{(1)}, \quad (2.20)$$

$$\tilde{s}^{(2)} = \tilde{s}_{\text{bare}}^{(2)} - Z_s^{(2)} - \tilde{s}_{\text{bare}}^{(1)} Z_s^{(1)} + \left(Z_s^{(1)} \right)^2 - \frac{\beta_0}{\epsilon} \tilde{s}_{\text{bare}}^{(1)}. \quad (2.21)$$

All the divergences in the bare soft function \tilde{s}_{bare} are related to the renormalization constant Z_s and thus the anomalous dimensions according to the above discussions.

3 NLO soft function

The NLO bare soft function can be obtained by calculating the integral

$$s_{\text{bare}}^{(1)}(\tau, \mu, \beta, y) = -\frac{2e^{\gamma_E\epsilon}\mu^{2\epsilon}}{\pi^{1-\epsilon}} \int d^d k \delta(k^2) \theta(k^0) J_a^{\mu(0)\dagger}(k) J_{a\mu}^{(0)}(k) F(v_1, v_2, k), \quad (3.1)$$

where the leading order soft current is defined as

$$J_a^{\mu(0)}(k) = -\sum_{i=1}^3 \mathbf{T}_i^a \frac{v_i^\mu}{v_i \cdot k}. \quad (3.2)$$

A prefactor $e^{\gamma_E\epsilon}(4\pi)^{-\epsilon}$ has been inserted due to our choice of the $\overline{\text{MS}}$ scheme in renormalization of α_s . In eq. (3.1), $F(v_1, v_2, k)$ is the measurement function in the threshold limit, defined as

$$F(v_1, v_2, k) = \delta \left(\tau - \frac{1}{\sqrt{s_{12}}} (v_1 + v_2) \cdot k \right) = \sqrt{s_{12}} \delta(\omega - v_0 \cdot k). \quad (3.3)$$

With the Lorentz indices contracted, the NLO soft function is represented by

$$\begin{aligned} s_{\text{bare}}^{(1)}(\tau, \mu, \beta, y) = & -\frac{2e^{\gamma_E\epsilon}\mu^{2\epsilon}}{\pi^{1-\epsilon}} \sqrt{s_{12}} \int d^d k \delta(k^2) \theta(k^0) \delta(\omega - v_0 \cdot k) \\ & \times \left[\frac{2\mathbf{T}_1 \cdot \mathbf{T}_2 v_1 \cdot v_2}{(v_1 \cdot k)(v_2 \cdot k)} + \frac{2\mathbf{T}_1 \cdot \mathbf{T}_3 v_1 \cdot v_3}{(v_1 \cdot k)(v_3 \cdot k)} + \frac{2\mathbf{T}_2 \cdot \mathbf{T}_3 v_2 \cdot v_3}{(v_2 \cdot k)(v_3 \cdot k)} + \frac{\mathbf{T}_3 \cdot \mathbf{T}_3 v_3 \cdot v_3}{(v_3 \cdot k)^2} \right] \end{aligned}$$

$$= \tau^{-1-2\epsilon} \left(\frac{\mu^2}{s_{12}} \right)^\epsilon s_{\text{bare}}^{(1)}(\beta, y). \quad (3.4)$$

In the third line, we have written the dependence on τ and μ explicitly in the result. The color charges would act on the color bases of the hard function. Due to its simple color configuration, there is only one color basis up to all orders for the $bg \rightarrow tW$ process. Therefore we can make the substitution in the above equation:

$$\mathbf{T}_1 \cdot \mathbf{T}_2 \rightarrow -\frac{C_A}{2}, \quad \mathbf{T}_1 \cdot \mathbf{T}_3 \rightarrow \frac{C_A}{2} - C_F, \quad \mathbf{T}_2 \cdot \mathbf{T}_3 \rightarrow -\frac{C_A}{2}, \quad \mathbf{T}_3 \cdot \mathbf{T}_3 \rightarrow C_F \quad (3.5)$$

with $C_F = 4/3$ and $C_A = 3$ being the Casimir operators of $SU(3)$ in the fundamental and adjoint representations, respectively.

The first term in the integrand of eq. (3.4) depends only on v_1 and v_2 , and thus is easy to compute. The other terms depend on v_3 and deserve a detailed discussion. They can be represented by the integral family

$$F_{a_1, a_2} = \int [dk] \delta(\omega - v_0 \cdot k) \frac{1}{(v_1 \cdot k)^{a_1} (v_3 \cdot k)^{a_2}} \quad (3.6)$$

with $[dk] \equiv d^d k \delta(k^2) \theta(k^0)$. The result for the integral containing v_2 can be obtained by replacing y by $-y$. We treat the δ -functions by making use of the reverse unitary method to change them in the form of propagators, i.e.,

$$\delta(k^2) \theta(k^0) = \frac{1}{2\pi i} \left(\frac{1}{k^2 - i0^+} - \frac{1}{k^2 + i0^+} \right) \theta(k^0), \quad (3.7)$$

$$\delta(\omega - v_0 \cdot k) = \frac{1}{2\pi i} \left(\frac{1}{\omega - v_0 \cdot k - i0^+} - \frac{1}{\omega - v_0 \cdot k + i0^+} \right). \quad (3.8)$$

As a result, the integrals in this family can be reduced to a finite set of master integrals because of the relations among them derived from the IBP identities⁴. We have employed the package FIRE6, which implements the algorithms proposed in ref. [56], to perform the reduction, and found the following master integrals,

$$\vec{f}(\omega, \beta, y, \epsilon) = (F_{0,0}, F_{0,1}, F_{1,1})^T. \quad (3.9)$$

Then we calculate the master integrals analytically with the method of differential equations. In particular, we have transformed the differential equation into the canonical form [44]

$$\frac{\partial \vec{g}(\beta, y, \epsilon)}{\partial \beta} = \epsilon \hat{B}(\beta, y) \vec{g}(\beta, y, \epsilon) \quad (3.10)$$

by choosing a proper basis $\vec{g}(\beta, y, \epsilon) = \hat{T}(\omega, \beta, y, \epsilon) \vec{f}(\omega, \beta, y, \epsilon)$ with

$$\hat{T}(\omega, \beta, y, \epsilon) = \frac{2\Gamma(1-2\epsilon)}{\omega^{1-2\epsilon} \pi^{1-\epsilon} \Gamma(1-\epsilon)} \begin{pmatrix} 1-2\epsilon & 0 & 0 \\ 0 & \epsilon\omega\beta & 0 \\ 0 & 0 & \epsilon\omega^2(1-\beta y) \end{pmatrix}. \quad (3.11)$$

⁴The $\theta(k^0)$ term in eq. (3.7) does not affect the IBP identities because its derivative gives $\delta(k^0)$, which causes scaleless integrals.

Note that the new basis \vec{g} is dimensionless and thus does not depend on ω . The coefficient matrix \hat{B} is independent of the dimensional regulator, and can be expressed by

$$\hat{B}(\beta, y) = \frac{\hat{a}}{\beta - 1} + \frac{\hat{b}}{\beta} + \frac{\hat{c}}{\beta + 1} + \frac{\hat{d}}{\beta - 1/y} \quad (3.12)$$

with

$$\hat{a} = \begin{pmatrix} 0 & 0 & 0 \\ -1 & -1 & 0 \\ -2 & -2 & 0 \end{pmatrix}, \quad \hat{b} = \begin{pmatrix} 0 & 0 & 0 \\ 0 & 2 & 0 \\ 4 & 0 & 2 \end{pmatrix}, \quad \hat{c} = \begin{pmatrix} 0 & 0 & 0 \\ 1 & -1 & 0 \\ -2 & 2 & 0 \end{pmatrix}, \quad \hat{d} = \begin{pmatrix} 0 & 0 & 0 \\ 0 & 0 & 0 \\ 0 & 0 & -2 \end{pmatrix}. \quad (3.13)$$

We are interested in the result of \vec{g} as an expansion in a series of ϵ ,

$$\vec{g}(\beta, y, \epsilon) = \sum_{n=0}^{\infty} \vec{g}^{(n)}(\beta, y) \epsilon^n, \quad (3.14)$$

where we have chosen deliberately the normalization factors of the basis integrals so that no negative powers of ϵ appear. Then we can solve the canonical differential equation order-by-order in ϵ ,

$$\vec{g}^{(n+1)}(\beta, y) = \int_0^\beta d\beta' \hat{B}(\beta', y) \vec{g}^{(n)}(\beta', y) + \vec{g}^{(n+1)}(0, y), \quad (3.15)$$

where $\vec{g}^{(n)}(0, y)$ is the boundary value.

Because there is no new divergence if setting the top quark at rest, the master integrals are regular at the phase space point of $\beta = 0$. Given that the transformation matrix \hat{T} is also regular, we derive the following regularity condition

$$0 = \lim_{\beta \rightarrow 0} \beta \partial_\beta \vec{g}(\beta, y, \epsilon) = \lim_{\beta \rightarrow 0} \beta \hat{B}(\beta, y) \vec{g}(\beta, y, \epsilon), \quad (3.16)$$

which leads to

$$\vec{g}(0, y, \epsilon) = (g_1, 0, -2g_1)^T. \quad (3.17)$$

Therefore, we only need to calculate the first basis integral g_1 , which is simple,

$$g_1(0, y, \epsilon) = \frac{2\Gamma(2-2\epsilon)}{\omega^{1-2\epsilon}\pi^{1-\epsilon}\Gamma(1-\epsilon)} \int [dk] \delta(\omega - v_0 \cdot k) = 1. \quad (3.18)$$

Another advantage of choosing the boundary condition in this way is that the master integrals at $\beta = 0$ do not depend on y . As a result, we do not have to construct and solve the differential equation with respect to y .

The full result of the basis integrals can be obtained using eq. (3.15), and can be written in terms of MPLs, which are defined by $G(\beta) = 1$ and

$$G(a_1, \dots, a_n; \beta) = \int_0^\beta \frac{dt}{t - a_1} G(a_2, \dots, a_n; t), \quad (3.19)$$

$$G(\vec{0}_n; \beta) = \frac{1}{n!} \ln^n \beta. \quad (3.20)$$

The MPLs have nice properties [57] and can be evaluated using the packages `GiNaC` [58] and `PolyLogTools` [59]. We provide the analytic results for all the basis integrals in an auxiliary file.

The NLO bare soft function in the Laplace space is

$$\tilde{s}_{\text{bare}}^{(1)}(t, \mu, \beta, y) = \Gamma(-2\epsilon) \left(\frac{\mu^2}{s_{12}t^2} \right)^\epsilon s_{\text{bare}}^{(1)}(\beta, y). \quad (3.21)$$

Performing renormalization according to eq. (2.20), we obtain the NLO renormalized soft function,

$$\begin{aligned} \tilde{s}^{(1)}(L, \beta, y) = & L^2(C_A + C_F) + L[2C_A(G_{-1/y} - G_{1/y}) + 2C_F(-1 - G_{-1} - G_1 + 2G_{1/y})] \\ & \frac{C_A}{6}(\pi^2 - 24G_{0,-1/y} + 24G_{0,1/y} - 12G_{-1/y,-1} - 12G_{-1/y,1} + 24G_{-1/y,-1/y} + 12G_{1/y,-1} \\ & + 12G_{1/y,1} - 24G_{1/y,1/y}) + \frac{C_F}{6} \left[\frac{12}{\beta}(G_{-1} - G_1) + \pi^2 - 12G_{-1,-1} + 12G_{-1,1} + 24G_{0,-1} \right. \\ & \left. + 24G_{0,1} - 48G_{0,1/y} + 12G_{1,-1} - 12G_{1,1} - 24G_{1/y,-1} - 24G_{1/y,1} + 48G_{1/y,1/y} \right], \end{aligned} \quad (3.22)$$

where $L = \ln \frac{s_{12}t^2}{\mu^2}$ and $G_{a_1, \dots, a_n} \equiv G(a_1, \dots, a_n; \beta)$.

4 NNLO soft function

The NNLO bare soft function consists of two parts, i.e., the double-real and virtual-real corrections, and thus can be expressed as

$$\begin{aligned} s_{\text{bare}}^{(2)}(\tau, \mu, \beta, y) &= s_{\text{DR}}^{(2)}(\tau, \mu, \beta, y) + s_{\text{VR}}^{(2)}(\tau, \mu, \beta, y) \\ &= \tau^{-1-4\epsilon} \left(\frac{\mu^2}{s_{12}} \right)^{2\epsilon} s_{\text{bare}}^{(2)}(\beta, y). \end{aligned} \quad (4.1)$$

The selected Feynman diagrams for the double-real corrections are shown in figure 1. Depending on the final state, this part splits further into two terms,

$$s_{\text{DR}}^{(2)}(\tau, \mu, \beta, y) = s_{gg}^{(2)}(\tau, \mu, \beta, y) + s_{q\bar{q}}^{(2)}(\tau, \mu, \beta, y). \quad (4.2)$$

The emission of two soft gluons contributes to the first term,

$$\begin{aligned} s_{gg}^{(2)}(\tau, \mu, \beta, y) = & \frac{2e^{2\gamma_E\epsilon}\mu^{4\epsilon}}{\pi^{2-2\epsilon}} \int d^d k_1 d^d k_2 \delta(k_1^2) \theta(k_1^0) \delta(k_2^2) \theta(k_2^0) \\ & \times J_{a_1 a_2}^{\mu_1 \nu_1(0)\dagger}(k_1, k_2) d_{\mu_1 \mu_2}(k_1) d_{\nu_1 \nu_2}(k_2) J_{a_1 a_2}^{\mu_2 \nu_2(0)}(k_1, k_2) F(v_1, v_2, k_1, k_2), \end{aligned} \quad (4.3)$$

where the two-gluon soft current is given by [60, 61]

$$J_{a_1 a_2}^{\mu\nu(0)}(k_1, k_2) = \frac{1}{2} \left\{ J_{a_1}^{\mu(0)}, J_{a_2}^{\nu(0)} \right\} + i f_{a_1 a_2 a_3} \sum_{i=1}^3 \mathbf{T}_i^{a_3} \quad (4.4)$$

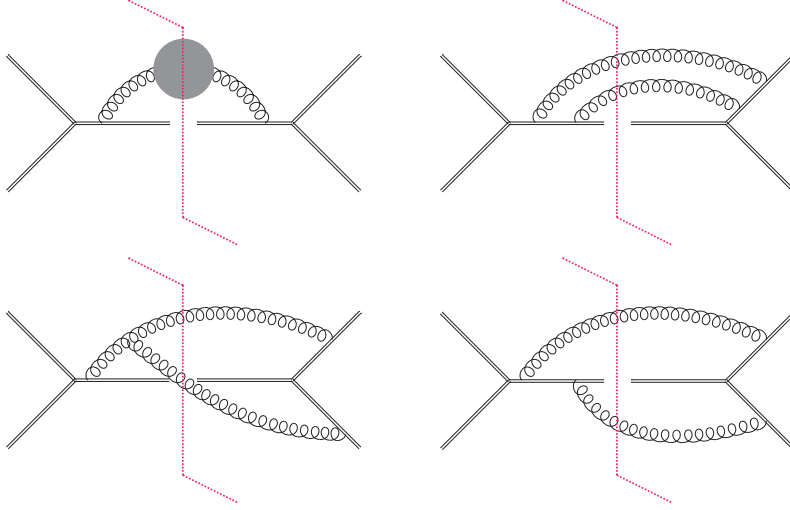


Figure 1: Sample double-real diagrams contributing to the NNLO soft function. The blob in the first diagram denotes the gluon self-energy subgraph.

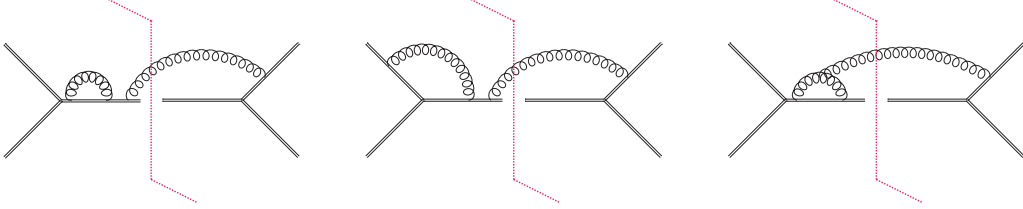


Figure 2: Sample virtual-real diagrams contributing to the NNLO soft function.

$$\times \left[\frac{v_i^\mu k_1^\nu - v_i^\nu k_2^\mu}{k_1 \cdot k_2 v_i \cdot (k_1 + k_2)} - \frac{v_i \cdot (k_1 - k_2)}{2v_i \cdot (k_1 + k_2)} \left(\frac{v_i^\mu v_i^\nu}{v_i \cdot k_1 v_i \cdot k_2} + \frac{g^{\mu\nu}}{k_1 \cdot k_2} \right) \right].$$

Because of current conservation, one can take the polarization tensor $d_{\mu_1\mu_2} = -g_{\mu_1\mu_2}$ for simplicity. The second term in eq. (4.2) represents the effect of a soft quark-antiquark pair,

$$s_{q\bar{q}}^{(2)}(\tau, \mu, \beta, y) = \frac{2e^{2\gamma_E\epsilon}\mu^{4\epsilon}}{\pi^{2-2\epsilon}} \int [dk_1][dk_2] \sum_{i,j=1}^3 \mathcal{T}_{ij}(k_1, k_2) F(v_1, v_2, k_1, k_2) \quad (4.5)$$

with

$$\mathcal{T}_{ij}(k_1, k_2) = -\mathbf{T}_F \mathbf{T}_i \cdot \mathbf{T}_j \frac{2v_i \cdot v_j k_1 \cdot k_2 + v_i \cdot (k_1 - k_2) v_j \cdot (k_1 - k_2)}{2(k_1 \cdot k_2)^2 v_i \cdot (k_1 + k_2) v_j \cdot (k_1 + k_2)}, \quad (4.6)$$

which can be found in [60]. We have checked that these expressions can be reproduced from the expansion of the soft Wilson lines. In the case of double emissions, the measurement function $F(v_1, v_2, k_1, k_2)$ is defined as

$$F(v_1, v_2, k_1, k_2) = \sqrt{s_{12}} \delta(\omega - v_0 \cdot (k_1 + k_2)). \quad (4.7)$$

Figure 2 shows selected Feynman diagrams relevant to virtual-real corrections. Their contributions to the NNLO soft function can be written as

$$s_{\text{VR}}^{(2)}(\tau, \mu, \beta, y) = \frac{4e^{2\gamma_E\epsilon}\mu^{4\epsilon}}{\pi^{1-\epsilon}} \text{Re} \left[\int [dk] J_a^{\mu(0)\dagger}(k) J_{a\mu}^{(1)}(k) F(v_1, v_2, k) \right]. \quad (4.8)$$

The analytic result of the one-loop soft current $J_a^{\nu(1)}(k)$ can be found in [62]. However, it is not suitable for performing the integration over k . Therefore, we use the form of $J_a^{\nu(1)}(k)$ with the soft loop momentum l unintegrated.

The scalar integrals needed in the calculation of double-real corrections can be written as

$$F_{a_1, a_2, a_3, a_4, a_5, a_6}^{(i)} = \int [dk_1] [dk_2] \delta(\omega - v_0 \cdot (k_1 + k_2)) \prod_{j=1}^6 \frac{1}{(D_j^{(i)})^{a_j}}, \quad (4.9)$$

where $D_j^{(i)}$ is the j -th denominator in the i -th family. After performing reduction, we find two integral families with the following denominators:

$$D_j^{(1)} : \quad v_1 \cdot k_2, \quad v_1 \cdot (k_1 + k_2), \quad v_2 \cdot k_1, \quad v_3 \cdot k_1, \quad v_3 \cdot (k_1 + k_2), \quad (k_1 + k_2)^2, \quad (4.10)$$

$$D_j^{(2)} : \quad v_1 \cdot k_1, \quad v_1 \cdot k_2, \quad v_2 \cdot k_1, \quad v_3 \cdot k_1, \quad v_3 \cdot k_2, \quad (k_1 + k_2)^2. \quad (4.11)$$

There are 13 and 12 master integrals for the first and second families, respectively, which can be chosen as

$$\vec{f}^{(1)}(\omega, \beta, y, \epsilon) = (F_{0,0,0,0,0,0}^{(1)}, F_{0,0,0,1,0,0}^{(1)}, F_{0,0,0,0,1,0}^{(1)}, F_{0,0,0,1,1,0}^{(1)}, F_{1,0,0,0,1,0}^{(1)}, F_{1,0,0,1,1,0}^{(1)}, \\ F_{1,0,0,1,0,1}^{(1)}, F_{1,0,0,1,-1,1}^{(1)}, F_{0,1,0,1,0,0}^{(1)}, F_{0,1,0,0,1,0}^{(1)}, F_{-1,1,0,1,0,0}^{(1)}, F_{1,-1,0,1,0,1}^{(1)}, F_{1,1,0,1,1,0}^{(1)})^T,$$

and

$$\vec{f}^{(2)}(\omega, \beta, y, \epsilon) = (F_{0,0,0,0,0,0}^{(2)}, F_{0,0,0,1,0,0}^{(2)}, F_{0,0,1,1,0,0}^{(2)}, F_{1,0,0,1,0,0}^{(2)}, F_{0,0,0,0,1,0}^{(2)}, F_{0,1,0,0,1,0}^{(2)}, \\ F_{0,0,0,1,1,0}^{(2)}, F_{1,0,0,1,1,0}^{(2)}, F_{0,1,0,1,1,0}^{(2)}, F_{0,0,1,1,1,0}^{(2)}, F_{0,1,1,1,1,0}^{(2)}, F_{1,1,0,1,1,0}^{(2)})^T. \quad (4.12)$$

The scalar integrals for virtual-real corrections can be written as

$$F_{a_1, a_2, a_3, a_4, a_5, a_6, a_7}^{(3)} = \int [dk] d^d l \delta(\omega - v_0 \cdot k) \prod_{j=1}^7 \frac{1}{(D_j^{(3)})^{a_j}} \quad (4.13)$$

with the denominators

$$D_j^{(3)} : \quad v_1 \cdot k, \quad v_1 \cdot l, \quad v_2 \cdot (k - l), \quad v_3 \cdot k, \quad v_3 \cdot (k - l), \quad l^2, \quad (k - l)^2. \quad (4.14)$$

All the scalar integrals are reduced to 9 master integrals,

$$\vec{f}^{(3)}(\omega, \beta, y, \epsilon) = (F_{0,1,0,0,1,0,1}^{(3)}, F_{-1,0,0,0,1,1,0}^{(3)}, F_{0,0,0,0,1,1,0}^{(3)}, F_{1,0,0,0,1,1,0}^{(3)}, F_{0,1,0,0,1,1,1}^{(3)},$$

$$F_{-1,1,0,0,1,1,1}^{(3)}, F_{0,1,0,-1,1,1,1}^{(3)}, F_{-1,1,0,1,1,0,1}^{(3)}, F_{0,1,0,1,1,0,1}^{(3)})^T. \quad (4.15)$$

To obtain the canonical basis, we have conducted a linear transformation on $\vec{f}^{(i)}$, i.e., $\vec{g}^{(i)}(\epsilon, \beta, y) = \hat{T}^{(i)}(\epsilon, \beta, y, \omega) \vec{f}^{(i)}(\epsilon, \beta, y, \omega)$, using the **Libra** package [63]. The differential equation of $\vec{g}^{(i)}$ is given by

$$\frac{\partial \vec{g}^{(i)}}{\partial \beta}(\beta, y, \epsilon) = \epsilon \left(\frac{\hat{a}^{(i)}}{\beta - 1} + \frac{\hat{b}^{(i)}}{\beta} + \frac{\hat{c}^{(i)}}{\beta + 1} + \frac{\hat{d}^{(i)}}{\beta - 1/y} + \frac{\hat{e}^{(i)}}{\beta + 1/y} \right) \vec{g}^{(i)}(\beta, y, \epsilon). \quad (4.16)$$

The explicit forms of the canonical basis and constant matrices in the numerators are collected in a supplementary file.

As in the case at NLO, we choose the point $\beta = 0$ as the boundary. The regularity condition requires that the bases have the following structures

$$\vec{g}^{(1)}(0, y, \epsilon) = \left(g_1^{(1)}, 0, 0, 0, 0, 0, \right. \\ \left. -\frac{12}{y}g_1^{(1)}, 6g_1^{(1)}, g_9^{(1)}, 0, \frac{1}{y}g_1^{(1)} - \frac{1}{4y}g_9^{(1)}, 0, \frac{4}{y^2}g_1^{(1)} + \frac{2}{y^2}g_9^{(1)} \right)^T, \quad (4.17)$$

$$\vec{g}^{(2)}(0, y, \epsilon) = \left(g_1^{(2)}, 0, 2g_1^{(2)}, -2g_1^{(2)}, 0, -2g_1^{(2)}, 0, 0, 0, 0, -24g_1^{(2)}, g_1^{(2)} \right)^T, \quad (4.18)$$

$$\vec{g}^{(3)}(0, y, \epsilon) = \left(g_1^{(3)}, g_2^{(3)}, 0, -\frac{96}{3+2y}g_2^{(3)}, \frac{320}{y^2(3-2y)} \left(\frac{2}{3}g_1^{(3)} - g_2^{(3)} \right), \right. \\ \left. 0, \frac{160}{y(3+2y)} \left(-\frac{2}{3}g_1^{(3)} + g_2^{(3)} \right), \frac{16(1+y-y^2)}{3y^2(3+2y)}g_1^{(3)}, 0 \right)^T. \quad (4.19)$$

After performing the phase space and loop integrations, we obtain the results of the boundary integrals,

$$g_1^{(1)}(0, y, \epsilon) = \frac{4\Gamma(4-4\epsilon)}{\omega^{3-4\epsilon}\pi^{2-2\epsilon}\Gamma^2(1-\epsilon)} \int [dk_1][dk_2] \delta(\omega - v_0 \cdot k_1 - v_0 \cdot k_2) = 1, \quad (4.20)$$

$$g_9^{(1)}(0, y, \epsilon) = \frac{4\Gamma(3-4\epsilon)}{\omega^{1-4\epsilon}\pi^{2-2\epsilon}\Gamma^2(-\epsilon)(1-2\epsilon)} \int [dk_1][dk_2] \frac{\delta(\omega - v_0 \cdot k_1 - v_0 \cdot k_2)}{[v_1 \cdot (k_1 + k_2)](v_3 \cdot k_1)} \\ = \frac{4\epsilon^2}{(1-2\epsilon)(1-3\epsilon)} {}_3F_2(1, 1-2\epsilon, 1-\epsilon; 2-3\epsilon, 2-2\epsilon; 1), \quad (4.21)$$

$$g_1^{(2)}(0, y, \epsilon) = g_1^{(1)}(0, y, \epsilon) = 1, \quad (4.22)$$

$$g_1^{(3)}(0, y, \epsilon) = \frac{i}{\pi^{3-2\epsilon}\omega^{1-4\epsilon}e^{2i\pi\epsilon}} \frac{\epsilon(1-4\epsilon)\Gamma(1-2\epsilon)}{\Gamma(2\epsilon)\Gamma^2(1-\epsilon)} \int [dk] d^d l \frac{\delta(\omega - v_0 \cdot k)}{(v_1 \cdot l)[v_3 \cdot (k-l)](k-l)^2} \\ = -e^{-2i\pi\epsilon} \frac{\Gamma(1-3\epsilon)\Gamma^2(1-2\epsilon)\Gamma(1+\epsilon)}{\Gamma(1-4\epsilon)\Gamma^2(1-\epsilon)}, \quad (4.23)$$

$$g_2^{(3)}(0, y, \epsilon) = -\frac{i}{\pi^{3-2\epsilon}\omega^{2-4\epsilon}e^{2i\pi\epsilon}} \frac{(1-2\epsilon)\Gamma(2-2\epsilon)}{\Gamma(2\epsilon)\Gamma^2(1-\epsilon)} \int [dk] d^d l \frac{\delta(\omega - v_0 \cdot k)}{[v_3 \cdot (k-l)]l^2} = 1, \quad (4.24)$$

where the hypergeometric function in eq. (4.21) can be expanded order-by-order in ϵ by using the package **HypExp** [64]. These results agree with those in ref. [65]⁵.

⁵There is a typo in ref. [65] for the result of the integral in eq. (4.21).

With these boundary values, it is ready to solve the differential equation (4.16) and the canonical bases $\bar{g}^{(i)}$ can be expressed in terms of MPLs. Note that there are still two master integrals which do not depend on β . Thus, they cannot be calculated using differential equations. Instead, they can be evaluated directly,

$$\begin{aligned} F_{1,0,1,0,0,1}^{(1)} &= \int [dk_1] [dk_2] \frac{\delta(\omega - v_0 \cdot k_1 - v_0 \cdot k_2)}{(v_1 \cdot k_2)(v_2 \cdot k_1)} \frac{1}{(k_1 + k_2)^2} \\ &= \pi^{2-2\epsilon} \omega^{-1-4\epsilon} \frac{1}{(2\epsilon)^2} \frac{\Gamma^2(-2\epsilon) \Gamma(-\epsilon)}{\Gamma(-3\epsilon) \Gamma(-4\epsilon)} {}_3F_2(-\epsilon, -\epsilon, -\epsilon; 1-\epsilon, -3\epsilon; 1), \end{aligned} \quad (4.25)$$

$$\begin{aligned} F_{0,1,1,0,0,1,1}^{(3)} &= \int [dk] d^d l \frac{\delta(\omega - v_0 \cdot k)}{(v_1 \cdot l) [v_2 \cdot (k-l)] l^2 (k-l)^2} \frac{1}{l^2 (k-l)^2} \\ &= -\frac{i\pi^{3-2\epsilon} \omega^{-1-4\epsilon} e^{i\pi\epsilon}}{2} \frac{\Gamma(1+\epsilon) \Gamma(\epsilon) \Gamma^2(-\epsilon) \Gamma(-2\epsilon)}{\Gamma(-4\epsilon)}. \end{aligned} \quad (4.26)$$

For the first integral, we have utilized the trick to insert a $\delta^{(d)}(q - k_1 - k_2)$ function as suggested in ref. [66].

The NNLO soft function in Laplace space is given by

$$\tilde{s}_{\text{bare}}^{(2)}(t, \mu, \beta, y) = \Gamma(-4\epsilon) \left(\frac{\mu^2}{s_{12} t^2} \right)^{2\epsilon} s_{\text{bare}}^{(2)}(\beta, y). \quad (4.27)$$

All the divergences can be removed after performing renormalization according to eq. (2.21). We have also checked that the renormalized soft function $\tilde{s}(L, \beta, y)$ satisfies the scale evolution equation (2.14). The analytical expression of $\tilde{s}^{(2)}(L, \beta, y)$ is quite lengthy and can be found in the auxiliary file.

5 Asymptotic expansions and numerical results

In the limit of $\beta \rightarrow 0$, the NLO renormalized soft function reads

$$\tilde{s}^{(1)}(L, \beta \rightarrow 0, y) = L^2(C_A + C_F) - 2LC_F + \frac{\pi^2}{6}(C_A + C_F) + 4C_F + \mathcal{O}(\beta). \quad (5.1)$$

And the NNLO soft function is given by

$$\begin{aligned} \tilde{s}^{(2)}(L, \beta \rightarrow 0, y) &= L^4 \frac{(C_A + C_F)^2}{2} + L^3 \left[-\frac{11}{9}C_A^2 - 2C_F^2 - \frac{29}{9}C_A C_F + \frac{4}{9}(C_A + C_F)n_f T_F \right] \\ &+ L^2 \left[C_A^2 \left(\frac{67}{9} - \frac{\pi^2}{6} \right) + C_F^2 \left(6 + \frac{\pi^2}{6} \right) + \frac{136}{9}C_A C_F - \frac{4}{9}(5C_A + 8C_F)n_f T_F \right] \\ &+ L \left[C_A^2 \left(-\frac{404}{27} + 14\zeta_3 \right) + C_F^2 \left(-8 - \frac{\pi^2}{3} \right) + C_A C_F \left(-\frac{1094}{27} + \frac{\pi^2}{3} + 10\zeta_3 \right) \right. \\ &+ \left. \frac{8}{27}(14C_A + 47C_F)n_f T_F \right] + C_A^2 \left(\frac{1214}{81} + \frac{67\pi^2}{108} - \frac{11\pi^4}{72} - \frac{11\zeta_3}{9} \right) \\ &+ C_F^2 \left(8 + \frac{2\pi^2}{3} + \frac{\pi^4}{72} \right) + C_A C_F \left(\frac{5918}{81} + \frac{211\pi^2}{108} - \frac{\pi^4}{15} - \frac{101\zeta_3}{9} \right) \end{aligned}$$

$$-\frac{1}{81} \left[C_A (328 + 15\pi^2 - 36\zeta_3) + C_F (2248 + 15\pi^2 - 36\zeta_3) \right] n_f T_F + \mathcal{O}(\beta). \quad (5.2)$$

No singular $1/\beta$ or $\log \beta$ terms appear, which agrees with the expectation that no new divergences, e.g., infrared or Coulomb divergences, arise when taking $\beta \rightarrow 0$. In addition, we find that there is no dependence on y in this limit because the top quark and W boson are produced at rest in the center-of-mass frame of the incoming partons.

On the other hand, in the limit of $\beta \rightarrow 1$, the top quark is highly boosted. Consequently, new collinear divergences would appear and are embodied in the form of $\ln^i(1-\beta)$. The NLO soft function becomes

$$\begin{aligned} \tilde{s}^{(1)}(L, \beta \rightarrow 1, y) = & -C_F \ln^2(1-\beta) - 2C_F(L+1-\ln 2)\ln(1-\beta) + L^2(C_A + C_F) \\ & + 2L \left[-C_F(1+\ln 2) + (2C_F - C_A)\ln(1-y) + C_A \ln(1+y) \right] + (C_A - C_F) \frac{5\pi^2}{6} \\ & + C_F(2\ln 2 - \ln^2 2) + (2C_F - C_A)\ln^2(1-y) + C_A \ln^2(1+y) - 2C_A \ln(1-y)\ln(1+y) \\ & + 4(C_A - C_F) \left[-\text{Li}_2\left(\frac{1}{1-y}\right) - \text{Li}_2(1+y) + \text{Li}_2\left(\frac{1+y}{1-y}\right) \right] + \mathcal{O}(1-\beta), \end{aligned} \quad (5.3)$$

where we have converted MPLs into the dilogarithm and logarithm functions. We also note the singularities at $y = \pm 1$ in the above result. The $y = -1$ singularity corresponds to the phase space where the final-state top quark becomes collinear with the initial-state gluon. In this case, one should take it as a contribution from a collinear parton splitting convoluted with the partonic process $\bar{t}/t + b/\bar{b} \rightarrow W^-/W^+$, which means that the top quark must be considered as a parton inside the colliding proton. The $y = 1$ singularity actually exists only at a superficial level. It appears from the expansion of the terms like $1/\epsilon^2 \times (1-y)^{-\epsilon}$. No such singularity remains if we take the limit $y \rightarrow 1$ firstly⁶. We emphasize that these singularities appear only at the corner of $\beta = 1$ and $y = \pm 1$. Thus they can be neglected when we focus on the phenomenology at a real collider.

The NNLO soft function in the $\beta \rightarrow 1$ limit can be found in the auxiliary file. Below we only present the terms with $\ln^i(1-\beta)$, $i = 4, 3, 2$, to exhibit its structure:

$$\begin{aligned} \tilde{s}^{(2)}(L, \beta \rightarrow 1, y) = & \frac{C_F^2}{2} \ln^4(1-\beta) + C_F \left[\frac{11}{9} C_A + 2C_F(L+1-\ln 2) - \frac{4}{9} n_f T_F \right] \ln^3(1-\beta) \\ & + C_F \left\{ L^2(C_F - C_A) + L \left[\frac{11}{3} C_A + 2C_F(3-\ln 2) - \frac{4}{3} n_f T_F + 2(C_A - 2C_F)\ln(1-y) \right. \right. \\ & \left. \left. - 2C_A \ln(1+y) \right] + C_A \left[-\frac{34}{9} - \frac{\pi^2}{2} - \frac{11}{3} \ln 2 - \ln^2(1+y) + 2\ln(1-y)\ln(1+y) \right] \right. \\ & \left. + C_F \left(2 + \frac{5\pi^2}{6} - 6\ln 2 + 3\ln^2 2 \right) + \frac{4}{9} n_f T_F (2 + 3\ln 2) + (C_A - 2C_F)\ln^2(1-y) \right. \\ & \left. + 4(C_A - C_F) \left[\text{Li}_2\left(\frac{1}{1-y}\right) + \text{Li}_2(1+y) - \text{Li}_2\left(\frac{1+y}{1-y}\right) \right] \right\} \ln^2(1-\beta) + \dots \end{aligned} \quad (5.4)$$

⁶This argument cannot be extended to the $y = -1$ singularity because the hard function contains the $1/(1+y)$ pole.

In figure 3, we show the soft function as a function of the velocity β and the angular parameter y . The numerical result is calculated using $n_f = 5$, $T_F = 1/2$ and $L = 0$. It can be seen that the soft function varies slowly in the region of $\beta < 0.8$ and $y > -0.5$. When y becomes smaller, the soft function increases. When β approaches 1, the soft function changes dramatically due to the structure shown in eqs. (5.3) and (5.4). The NLO and NNLO soft functions exhibit similar shapes.

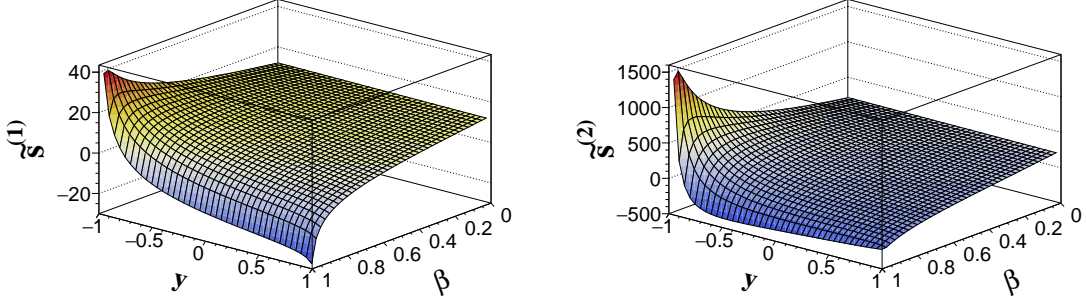


Figure 3: Pure NLO (left) and pure NNLO (right) soft functions as a function of β and y .

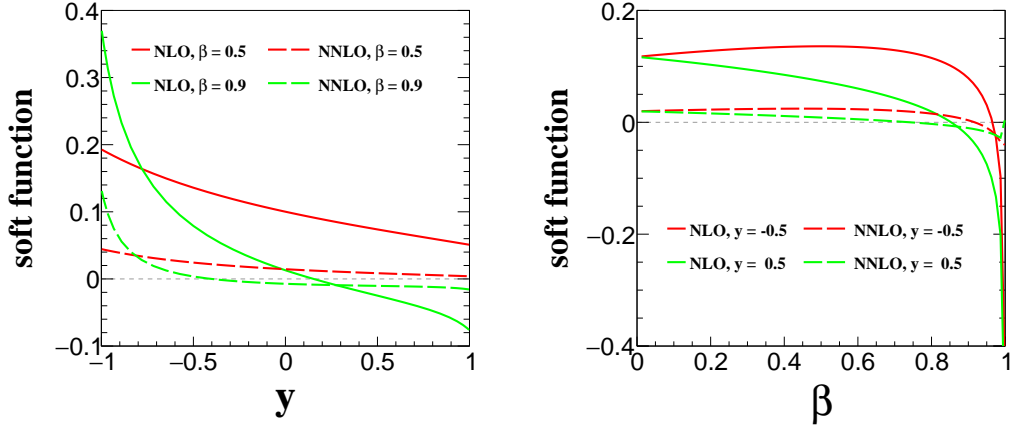


Figure 4: Pure NLO and pure NNLO soft functions, corresponding to eq. (2.20) and eq. (2.21), respectively, at fixed values of β (left) or y (right).

To see the impact of the soft function more clearly, we show the 2-dimensional plots with fixed values of β or y in figure 4. We have multiplied the expansion parameter $(\alpha_s/4\pi)^i$, $i = 1, 2$, for the NLO and NNLO soft functions, respectively, and taken $\alpha_s = 0.118$ in numerical calculation. In the case of $\beta = 0.5$, the NLO soft function changes from 0.2 to 0.05 as y varies from -1 to 1 , and the NNLO soft function provides a correction of about $23\% - 8\%$ depending on the value of y . When setting $\beta = 0.9$, we see a significant change in the NLO soft function; it changes from positive to negative values with the increasing of y . The NNLO soft function has a similar distribution but the magnitude is much smaller.

We have also fixed the value of y to demonstrate the variation with respect to β . For $y = -0.5$, the soft function is stable against the change of β except for the region near $\beta = 1$, and the NNLO correction is about 17% relative to the NLO result. For $y = 0.5$, the soft function decreases fast and becomes negative around $\beta = 0.85$.

6 Conclusions

In this paper, we compute the two-loop soft function for associated top quark and W boson production near threshold, which is a critical ingredient for achieving next-to-next-to-next-to-leading logarithmic resummation of soft-gluon effects. We have employed IBP reduction and the method of differential equations to calculate the master integrals. The divergences completely cancel out after performing the renormalization using the known anomalous dimension of the soft function, which validates our calculation. The full analytic results of the NLO and NNLO soft functions are expressed in terms of MPLs. The asymptotic behaviors of the soft function in the low-energy limit ($\beta \rightarrow 0$) and the high-energy limit ($\beta \rightarrow 1$) are also analyzed. Numerical results demonstrate the stability of the soft function in moderate kinematic regions and the rapid change in the high energy limit. Our results show that the NNLO corrections are around 10% – 20% with respect to the NLO soft function in the major part of the phase space.

Acknowledgement

This work was partly supported by the National Natural Science Foundation of China under grant No. 12275156, No. 12321005 and the Taishan Scholar Foundation of Shandong province (tsqn201909011). The Feynman diagrams were drawn using JaxoDraw [67].

References

- [1] ATLAS collaboration, G. Aad et al., *Evidence for the associated production of a W boson and a top quark in ATLAS at $\sqrt{s} = 7$ TeV*, *Phys. Lett. B* **716** (2012) 142–159, [[1205.5764](#)].
- [2] CMS collaboration, S. Chatrchyan et al., *Evidence for Associated Production of a Single Top Quark and W Boson in pp Collisions at $\sqrt{s} = 7$ TeV*, *Phys. Rev. Lett.* **110** (2013) 022003, [[1209.3489](#)].
- [3] CMS collaboration, S. Chatrchyan et al., *Observation of the associated production of a single top quark and a W boson in pp collisions at $\sqrt{s} = 8$ TeV*, *Phys. Rev. Lett.* **112** (2014) 231802, [[1401.2942](#)].
- [4] ATLAS collaboration, G. Aad et al., *Measurement of the production cross-section of a single top quark in association with a W boson at 8 TeV with the ATLAS experiment*, *JHEP* **01** (2016) 064, [[1510.03752](#)].
- [5] ATLAS collaboration, M. Aaboud et al., *Measurement of the cross-section for producing a W boson in association with a single top quark in pp collisions at $\sqrt{s} = 13$ TeV with ATLAS*, *JHEP* **01** (2018) 063, [[1612.07231](#)].

- [6] ATLAS collaboration, M. Aaboud et al., *Measurement of differential cross-sections of a single top quark produced in association with a W boson at $\sqrt{s} = 13$ TeV with ATLAS*, *Eur. Phys. J. C* **78** (2018) 186, [[1712.01602](#)].
- [7] CMS collaboration, A. M. Sirunyan et al., *Measurement of the production cross section for single top quarks in association with W bosons in proton-proton collisions at $\sqrt{s} = 13$ TeV*, *JHEP* **10** (2018) 117, [[1805.07399](#)].
- [8] CMS collaboration, A. Tumasyan et al., *Measurement of inclusive and differential cross sections for single top quark production in association with a W boson in proton-proton collisions at $\sqrt{s} = 13$ TeV*, *JHEP* **07** (2023) 046, [[2208.00924](#)].
- [9] ATLAS collaboration, G. Aad et al., *Measurement of single top-quark production in association with a W boson in pp collisions at $s=13$ TeV with the ATLAS detector*, *Phys. Rev. D* **110** (2024) 072010, [[2407.15594](#)].
- [10] CMS collaboration, A. Hayrapetyan et al., *Measurement of inclusive and differential cross sections of single top quark production in association with a W boson in proton-proton collisions at $\sqrt{s} = 13.6$ TeV*, *JHEP* **01** (2025) 107, [[2409.06444](#)].
- [11] ATLAS collaboration, M. Aaboud et al., *Probing the quantum interference between singly and doubly resonant top-quark production in pp collisions at $\sqrt{s} = 13$ TeV with the ATLAS detector*, *Phys. Rev. Lett.* **121** (2018) 152002, [[1806.04667](#)].
- [12] A. S. Belyaev, E. E. Boos and L. V. Dudko, *Single top quark at future hadron colliders: Complete signal and background study*, *Phys. Rev. D* **59** (1999) 075001, [[hep-ph/9806332](#)].
- [13] T. M. P. Tait, *The tW^- mode of single top production*, *Phys. Rev. D* **61** (1999) 034001, [[hep-ph/9909352](#)].
- [14] J. M. Campbell and F. Tramontano, *Next-to-leading order corrections to Wt production and decay*, *Nucl. Phys. B* **726** (2005) 109–130, [[hep-ph/0506289](#)].
- [15] S. Frixione, E. Laenen, P. Motylinski, B. R. Webber and C. D. White, *Single-top hadroproduction in association with a W boson*, *JHEP* **07** (2008) 029, [[0805.3067](#)].
- [16] F. Demartin, B. Maier, F. Maltoni, K. Mawatari and M. Zaro, *tWH associated production at the LHC*, *Eur. Phys. J. C* **77** (2017) 34, [[1607.05862](#)].
- [17] L. Dong, H. T. Li, Z.-Y. Li and J. Wang, *Subtraction of the $t\bar{t}$ contribution in $tW\bar{b}$ production at the one-loop level*, *JHEP* **01** (2025) 158, [[2411.07455](#)].
- [18] W. T. Giele, S. Keller and E. Laenen, *QCD corrections to W boson plus heavy quark production at the Tevatron*, *Phys. Lett. B* **372** (1996) 141–149, [[hep-ph/9511449](#)].
- [19] Q.-H. Cao, *Demonstration of One Cutoff Phase Space Slicing Method: Next-to-Leading Order QCD Corrections to the tW Associated Production in Hadron Collision*, [0801.1539](#).
- [20] P. Kant, O. M. Kind, T. Kintscher, T. Lohse, T. Martini, S. Mölbitz et al., *HatHor for single top-quark production: Updated predictions and uncertainty estimates for single top-quark production in hadronic collisions*, *Comput. Phys. Commun.* **191** (2015) 74–89, [[1406.4403](#)].
- [21] N. Kidonakis, *Single top production at the Tevatron: Threshold resummation and finite-order soft gluon corrections*, *Phys. Rev. D* **74** (2006) 114012, [[hep-ph/0609287](#)].
- [22] N. Kidonakis, *Two-loop soft anomalous dimensions for single top quark associated production with a W^- or H^-* , *Phys. Rev. D* **82** (2010) 054018, [[1005.4451](#)].

- [23] N. Kidonakis, *Soft-gluon corrections for tW production at N^3LO* , *Phys. Rev. D* **96** (2017) 034014, [[1612.06426](#)].
- [24] N. Kidonakis and N. Yamanaka, *Higher-order corrections for tW production at high-energy hadron colliders*, *JHEP* **05** (2021) 278, [[2102.11300](#)].
- [25] C. S. Li, H. T. Li, D. Y. Shao and J. Wang, *Momentum-space threshold resummation in tW production at the LHC*, *JHEP* **06** (2019) 125, [[1903.01646](#)].
- [26] E. Re, *Single-top Wt -channel production matched with parton showers using the POWHEG method*, *Eur. Phys. J. C* **71** (2011) 1547, [[1009.2450](#)].
- [27] T. Ježo, J. M. Lindert, P. Nason, C. Oleari and S. Pozzorini, *An $NLO+PS$ generator for $t\bar{t}$ and Wt production and decay including non-resonant and interference effects*, *Eur. Phys. J. C* **76** (2016) 691, [[1607.04538](#)].
- [28] L.-B. Chen and J. Wang, *Analytic two-loop master integrals for tW production at hadron colliders: I^** , *Chin. Phys. C* **45** (2021) 123106, [[2106.12093](#)].
- [29] M.-M. Long, R.-Y. Zhang, W.-G. Ma, Y. Jiang, L. Han, Z. Li et al., *Two-loop master integrals for the single top production associated with W boson*, [2111.14172](#).
- [30] J. Wang and Y. Wang, *Analytic two-loop master integrals for tW production at hadron colliders. Part II*, *JHEP* **02** (2023) 127, [[2211.13713](#)].
- [31] L.-B. Chen, L. Dong, H. T. Li, Z. Li, J. Wang and Y. Wang, *One-loop squared amplitudes for hadronic tW production at next-to-next-to-leading order in QCD*, *JHEP* **08** (2022) 211, [[2204.13500](#)].
- [32] L.-B. Chen, L. Dong, H. T. Li, Z. Li, J. Wang and Y. Wang, *Analytic two-loop QCD amplitudes for tW production: Leading color and light fermion-loop contributions*, *Phys. Rev. D* **106** (2022) 096029, [[2208.08786](#)].
- [33] L.-B. Chen, L. Dong, H. T. Li, Z. Li, J. Wang and Y. Wang, *Complete two-loop QCD amplitudes for tW production at hadron colliders*, *JHEP* **07** (2023) 089, [[2212.07190](#)].
- [34] H. T. Li and J. Wang, *Next-to-Next-to-Leading Order N -Jettiness Soft Function for One Massive Colored Particle Production at Hadron Colliders*, *JHEP* **02** (2017) 002, [[1611.02749](#)].
- [35] H. T. Li and J. Wang, *Next-to-next-to-leading order N -jettiness soft function for tW production*, *Phys. Lett. B* **784** (2018) 397–404, [[1804.06358](#)].
- [36] R. E. Cutkosky, *Singularities and discontinuities of Feynman amplitudes*, *J. Math. Phys.* **1** (1960) 429–433.
- [37] C. Anastasiou and K. Melnikov, *Higgs boson production at hadron colliders in NNLO QCD*, *Nucl. Phys. B* **646** (2002) 220–256, [[hep-ph/0207004](#)].
- [38] F. V. Tkachov, *A theorem on analytical calculability of 4-loop renormalization group functions*, *Phys. Lett. B* **100** (1981) 65–68.
- [39] K. G. Chetyrkin and F. V. Tkachov, *Integration by parts: The algorithm to calculate β -functions in 4 loops*, *Nucl. Phys. B* **192** (1981) 159–204.
- [40] A. V. Smirnov and F. S. Chukharev, *FIRE6: Feynman Integral REduction with modular arithmetic*, *Comput. Phys. Commun.* **247** (2020) 106877, [[1901.07808](#)].
- [41] A. V. Kotikov, *Differential equations method: New technique for massive Feynman diagrams calculation*, *Phys. Lett. B* **254** (1991) 158–164.

- [42] A. V. Kotikov, *Differential equation method: The Calculation of N point Feynman diagrams*, *Phys. Lett. B* **267** (1991) 123–127.
- [43] T. Gehrmann and E. Remiddi, *Differential equations for two-loop four-point functions*, *Nucl. Phys. B* **580** (2000) 485–518, [[hep-ph/9912329](#)].
- [44] J. M. Henn, *Multiloop integrals in dimensional regularization made simple*, *Phys. Rev. Lett.* **110** (2013) 251601, [[1304.1806](#)].
- [45] A. B. Goncharov, *Multiple polylogarithms, cyclotomy and modular complexes*, *arXiv e-prints* (May, 2011) [arXiv:1105.2076](#), [[1105.2076](#)].
- [46] T. Becher, M. Neubert and G. Xu, *Dynamical Threshold Enhancement and Resummation in Drell-Yan Production*, *JHEP* **07** (2008) 030, [[0710.0680](#)].
- [47] M. Beneke, A. P. Chapovsky, M. Diehl and T. Feldmann, *Soft collinear effective theory and heavy to light currents beyond leading power*, *Nucl. Phys. B* **643** (2002) 431–476, [[hep-ph/0206152](#)].
- [48] J. Chay, C. Kim, Y. G. Kim and J.-P. Lee, *Soft Wilson lines in soft-collinear effective theory*, *Phys. Rev. D* **71** (2005) 056001, [[hep-ph/0412110](#)].
- [49] G. P. Korchemsky and A. V. Radyushkin, *Infrared factorization, Wilson lines and the heavy quark limit*, *Phys. Lett. B* **279** (1992) 359–366, [[hep-ph/9203222](#)].
- [50] S. Catani and M. H. Seymour, *The Dipole formalism for the calculation of QCD jet cross-sections at next-to-leading order*, *Phys. Lett. B* **378** (1996) 287–301, [[hep-ph/9602277](#)].
- [51] S. Catani and M. H. Seymour, *A General algorithm for calculating jet cross-sections in NLO QCD*, *Nucl. Phys. B* **485** (1997) 291–419, [[hep-ph/9605323](#)].
- [52] A. Ferroglia, M. Neubert, B. D. Pecjak and L. L. Yang, *Two-loop divergences of massive scattering amplitudes in non-abelian gauge theories*, *JHEP* **11** (2009) 062, [[0908.3676](#)].
- [53] G. P. Korchemsky and G. Marchesini, *Structure function for large x and renormalization of Wilson loop*, *Nucl. Phys. B* **406** (1993) 225–258, [[hep-ph/9210281](#)].
- [54] S. Moch, J. A. M. Vermaseren and A. Vogt, *The Three loop splitting functions in QCD: The Nonsinglet case*, *Nucl. Phys. B* **688** (2004) 101–134, [[hep-ph/0403192](#)].
- [55] V. Ahrens, A. Ferroglia, M. Neubert, B. D. Pecjak and L. L. Yang, *Renormalization-Group Improved Predictions for Top-Quark Pair Production at Hadron Colliders*, *JHEP* **09** (2010) 097, [[1003.5827](#)].
- [56] S. Laporta, *High-precision calculation of multiloop Feynman integrals by difference equations*, *Int. J. Mod. Phys. A* **15** (2000) 5087–5159, [[hep-ph/0102033](#)].
- [57] C. Duhr, *Mathematical aspects of scattering amplitudes*, in *Theoretical Advanced Study Institute in Elementary Particle Physics: Journeys Through the Precision Frontier: Amplitudes for Colliders*, pp. 419–476, 2015, [[1411.7538](#), DOI].
- [58] C. W. Bauer, A. Frink and R. Kreckel, *Introduction to the GiNaC framework for symbolic computation within the C++ programming language*, *J. Symb. Comput.* **33** (2002) 1–12, [[cs/0004015](#)].
- [59] C. Duhr and F. Dulat, *PolyLogTools — polylogs for the masses*, *JHEP* **08** (2019) 135, [[1904.07279](#)].

- [60] S. Catani and M. Grazzini, *Infrared factorization of tree level QCD amplitudes at the next-to-next-to-leading order and beyond*, *Nucl. Phys. B* **570** (2000) 287–325, [[hep-ph/9908523](#)].
- [61] M. Czakon, *Double-real radiation in hadronic top quark pair production as a proof of a certain concept*, *Nucl. Phys. B* **849** (2011) 250–295, [[1101.0642](#)].
- [62] I. Bierenbaum, M. Czakon and A. Mitov, *The singular behavior of one-loop massive QCD amplitudes with one external soft gluon*, *Nucl. Phys. B* **856** (2012) 228–246, [[1107.4384](#)].
- [63] R. N. Lee, *Libra: A package for transformation of differential systems for multiloop integrals*, *Comput. Phys. Commun.* **267** (2021) 108058, [[2012.00279](#)].
- [64] T. Huber and D. Maitre, *HypExp 2, Expanding Hypergeometric Functions about Half-Integer Parameters*, *Comput. Phys. Commun.* **178** (2008) 755–776, [[0708.2443](#)].
- [65] G. Wang, X. Xu, L. L. Yang and H. X. Zhu, *The next-to-next-to-leading order soft function for top quark pair production*, *JHEP* **06** (2018) 013, [[1804.05218](#)].
- [66] T. Becher, G. Bell and S. Marti, *NNLO soft function for electroweak boson production at large transverse momentum*, *JHEP* **04** (2012) 034, [[1201.5572](#)].
- [67] D. Binosi, J. Collins, C. Kaufhold and L. Theussl, *JaxoDraw: A Graphical user interface for drawing Feynman diagrams. Version 2.0 release notes*, *Comput. Phys. Commun.* **180** (2009) 1709–1715, [[0811.4113](#)].